ANTICANCER RESEARCH *37*: 5693-5700 (2017)
doi:10.21873/anticanres.12006

Accurate Estimation of Functional Liver Volume Using Gd-EOB-DTPA MRI Compared to MDCT/^{99m}Tc-SPECT Fusion Imaging

YUJI MORINE*, CHINBOLD ENKHBOLD*, SATORU IMURA, TETSUYA IKEMOTO, SYUICHI IWAHASHI, YU SAITO, SHINICHIRO YAMADA, TOHRU UTSUNOMIYA and MITSUO SHIMADA

Department of Surgery, Institute of Biochemical Sciences, Tokushima University Graduate School, Tokushima, Japan

Abstract. *Background/Aim: We assessed the utility of dynamic magnetic resonance imaging (MRI) with gadoxetate-ethoxybenzyl-diethylenetriamine penta-aceticpenta-acetic acid (Gd-EOB-DTPA) (EOB-MRI) for estimating functional liver volume compared to ^{99m}Tc-galactosyl albumin single-photon-emission computed tomography (^{99m}Tc-GSA SPECT). Patients and Methods: Regional functional liver volume (left lateral, medial, right anterior, right posterior) of 58 hepatectomized patients was assessed using EOB-MRI and ^{99m}Tc-GSA SPECT, and compared to the actual liver volume with MDCT-3D volumetry. Results: ^{99m}Tc-GSA SPECT found a significantly lower functional volume of the left lateral section than the actual volume found by MDCT-3D volumetry (p=0.003) and EOB-MRI (p<0.001). Functional liver volume of right anterior section found with ^{99m}Tc-GSA SPECT was significantly higher than that found by MDCT-3D volumetry (p=0.04), despite no differences in asialoglycoprotein receptor 1 (ASGR1) or ATP-dependent organic anion transporting polypeptide 1 (OATP) expression between the left lateral and right anterior sections. Conclusion: ^{99m}Tc-GSA SPECT might underestimate the function of the left lobe and overestimate that of the right lobe. Therefore, EOB-MRI could be better for estimating the true regional functional liver reserve.*

Liver surgery remains the best treatment modality for liver cancer for offering the most favourable outcome (1). The mortality and morbidity rates after liver resection have declined in recent years owing to improved surgical techniques and imaging modalities (2-5), including preoperative volumetric analysis using three-dimensional (3D) imaging. The 3D imaging technique using several volumetric software packages based on computed tomographic (CT) data sets has permitted precise assessment of the actual remnant liver volume and anatomical information of the hepatic vasculature and biliary tract (6, 7). However, 3D-CT volumetry estimates only the actual liver volume, not the essential liver functional reserve.

^{99m}Tc-Galactosyl albumin (^{99m}Tc-GSA) scintigraphy has been reported to be a reliable diagnostic tool for estimating liver function and is useful for making the final decision regarding the extent of liver resection (8-11). Asialoglycoprotein receptor 1 (ASGR1) is a ^{99m}Tc-GSA-binding transmembrane molecule specifically expressed on the sinusoidal and basolateral hepatocellular membranes in normal liver (12). Recently, ^{99m}Tc-GSA scintigraphy has been combined with CT into a single-photon-emission CT (SPECT) system (13). The fusion image obtained with this system facilitates assessment of regional liver functional reserve with precise anatomical information (14-16). However, one report demonstrated the inaccuracy of CT/^{99m}Tc-GSA SPECT fusion image, in which the function of the left lobe was significantly lower compared to that of the right lobe in non-cirrhotic liver, and this divergence was considered the reason for the lower flow volume of the left portal vein compared to that in the right portal vein (17).

ATP-dependent organic anion transporting polypeptide 1 (OATP) is a liver-specific transporter located in the basolateral membrane of hepatocytes in normal liver (18). Gadoxetate-ethoxybenzyl-diethylenetriamine penta-acetic acid (Gd-EOB-DTPA) is a magnetic resonance imaging (MRI) contrast medium that is transported from the extracellular space into hepatocytes by OATP and is then secreted into biliary canaliculi. Thus, Gd-EOB-DTPA enhancement of the liver parenchyma depends on adequate liver function (19, 20). Recently, some studies have reported

*These Authors contributed equally to this study.

Correspondence to: Dr. Yuji Morine, Department of Surgery, Institute of Biochemical Sciences, Tokushima University Graduate School, 3-18-15 Kuramoto-cho, Tokushima 770-8503, Japan. Tel: +81 886339276, Fax: +81 886319698, e-mail: ymorine@tokushima-u.ac.jp

Key Words: EOB-MRI, asialoscintigraphy, functional liver volume, hepatectomy.

that MRI with Gd-EOB-DTPA (EOB-MRI) is highly sensitive and one of the standard imaging modalities that can be used to estimate liver function preoperatively (21-26). We also have reported that the liver function assessment method using EOB-MRI might represent a reliable and efficient imaging technique that could be used to estimate regional functional liver reserve in the clinical setting (27).

The current study aimed to compare the properties of EOB-MRI and ^{99m}Tc-GSA SPECT in assessing liver function and to demonstrate the possible utility of EOB-MRI over ^{99m}Tc-GSA SPECT for estimating the essential liver functional reserve in patients with non-cirrhotic liver who underwent liver surgery.

Patients and Methods

Patient selection. A total of 58 patients who underwent liver resection between 2008 and 2013 and were assessed preoperatively regarding their liver function with multidetector CT (MDCT), ^{99m}Tc-GSA scintigraphy, and EOB-MRI at the University of Tokushima were enrolled. Patients who had tumours of more than 3 cm, multiple tumours (more than four), central located tumours and those that made contact with the portal or biliary branch and involved vessels invasion were excluded. Patients with a cirrhotic liver were also excluded because of changes in liver haemodynamics of the portal flow. Patient characteristics are shown in Table I. The Institutional Review Board of the Tokushima University Graduate School authorized this study in advance (approval no.: 2478-1), and all patients provided written informed consent.

Table I. *Patient characteristics*.

Variable	n=58
Age (range), years	67.6±12.0 (38-85)
Gender: Male/female, n	42/16
HCV antibody-positive, n	21
HBs antigen-positive, n	15
Liver function data	
Platelet count (range), $\times 10^4/\mu l$	20.5±7.0 (10.0-39.8)
PT-INR (range)	0.96±0.08 (0.77-1.34)
PT (range), %	106.1±12.8 (62-150)
AST (range), IU/l	33.6±17.4 (11-79)
Total bilirubin (range), mg/dl	0.8±0.3 (0.1-2.3)
Albumin (range), g/dl	4.0±0.4 (2.9-4.9)
ICGR15 (range), %	9.8±4.6 (0.8-18.7)
Type of tumour, n	
Hepatocellular carcinoma	42
Cholangiocellular carcinoma	3
Metastatic tumour	10
Benign tumor	3
Tumor size (range), cm	2.3 (0.5-3.0)

HCV: Hepatitis C virus; HBs: hepatitis B surface; PT: prothrombin time; PT-INR: prothrombin international normalized ratio; AST: aspartate transaminase; ICGR15: indocyanine green dye retention at 15 min.

Imaging technique of MDCT. MDCT examinations were performed using an Aquilion 16 instrument (Toshiba Medical Systems Corporation, Tochigi, Japan). We adopted a multiphase CT protocol to acquire three image sets of the liver (arterial, portal, and equilibrium phases). The scans for each phase were acquired at 15 s (arterial), 30 s (portal), and 180 s (equilibrium phase) after administration of the nonionic contrast material iopamidol (Iopamiron 370; Nihon Schering, Osaka, Japan) at a rate of 3 ml/s.

Imaging technique of ^{99m}Tc-GSA scintigraphy. GSA imaging was performed as described previously (27). Briefly, after injecting 3 mg (185 MBq) of ^{99m}Tc-GSA (Nihon Medi-Physics, Nishinomiya, Japan), dynamic imaging was performed using a large field-of-view gamma camera. Regions of interest (ROIs) were defined for the liver and heart using standard imaging software, which was then used to create time–activity data. After ^{99m}Tc-GSA injection into an antecubital vein, dynamic SPECT acquisition was performed with a circular orbit by means of dual detectors equipped with a low-energy, high-resolution collimator. The acquisition time was 30 min (30 rotations).

Imaging technique of EOB-MRI. MRI was performed as described previously (27), using a superconducting magnet operating at 1.5T (Signa EXCITE HD; GE Medical Systems, Milwaukee, WI, USA) and an eight-channel phased-array coil. Gd-EOB-DTPA (0.1 mg/kg body weight) was administered intravenously as a bolus dose at a rate of 3 ml/s through an intravenous cubital line (20-22 gauge) that was flushed with 20 ml saline using a power injector. The hepatocyte-phase images obtained 20 min after injection were used for functional evaluation in this study. The images were acquired in the transverse plane and had a section thickness of 5 mm and a 2.5-mm overlap (*i.e.* 2.5-mm interval). Repetition time/echo time was 3.8/1.9 ms; flip angle was 12˚; number of signals acquired was 1; field of view was 38-40×38-40 cm; matrix was 320×192; and acquisition time was 18 s.

Data processing of functional liver volume with ^{99m}Tc-GSA SPECT. The functional liver volumetric calculation was made using data from contrast-enhanced MDCT and ^{99m}Tc-GSA SPECT with Synapse Vincent software (Fujifilm Medical Co. Ltd., Tokyo, Japan). The whole liver, portal vein, hepatic artery, and hepatic vein were extracted from the MDCT scans. After obtaining the image of the liver on MDCT, the whole liver volume was calculated automatically. We also calculated the actual and functional liver volume (%) separately in four sections (left lateral, medial, right anterior, right posterior) by the portal vein branch and depicted the MDCT image (Figure 1A) and MDCT/^{99m}Tc-GSA SPECT fusion image (Figure 1B). In this study, S1 (caudate lobe) evaluation by ^{99m}Tc-GSA SPECT was excluded because its volume too small for EOB-MRI evaluation in some cases and could not be compared between those modalities.

Data processing of functional liver volume with EOB-MRI. The signal intensities (SIs) of seven out of the eight Couinaud's segments (S2-S8) of the liver were measured using a circular ROI (approximately 100 mm^2) while avoiding major intrahepatic vessels. The caudate lobe was also excluded from this analysis. The SI of the right erector spina muscle was also measured at the level of the *porta hepatis*. ROI acquisition was performed using a commercially available picture archiving and communication system (Synapse; Fujifilm Medical, Tokyo, Japan). The relative SI for each patient

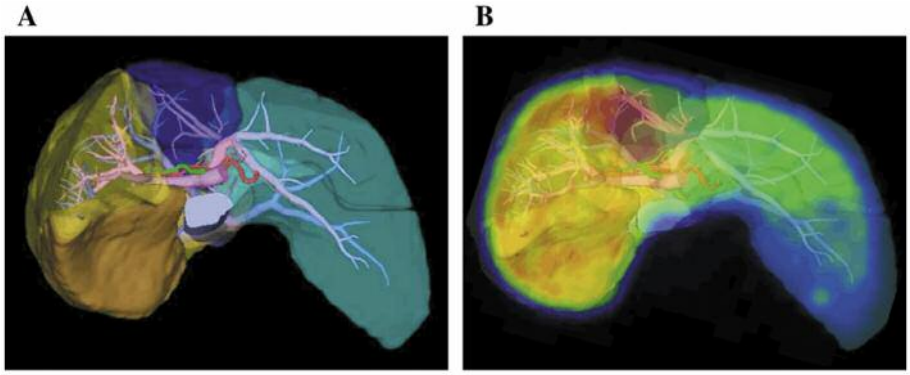

Figure 1. *Each liver section (left lateral, medial, right anterior, right posterior) was extracted from multidetector computed tomography (MDCT) three-dimensional volumetry (A) and MDCT/^{99m}Tc-galactosyl albumin single-photon-emission computed tomography fusion imaging (B).*

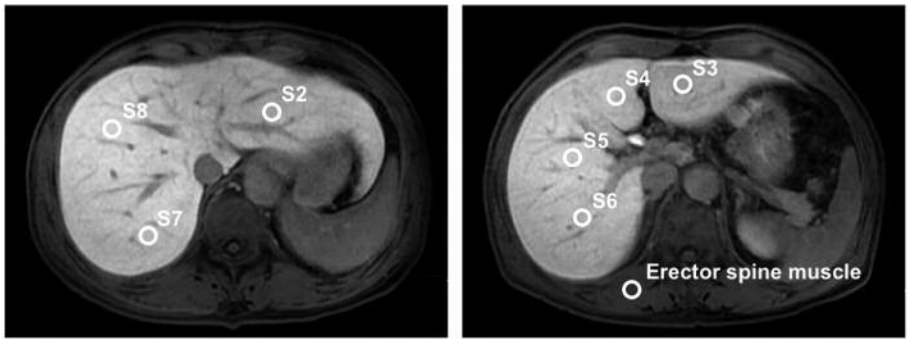

Figure 2. *The signal intensities in magnetic resonance images of the liver parenchyma were calculated by setting the seven regions of interest according to Couinaud's segments.*

was calculated as follows: relative SI=mean SI of each of the seven Couinaud's segments (S2-S8)/SI of muscle (Figure 2).

The corrected functional liver volume (%) in four sections (left lateral, medial, right anterior, right posterior) using EOB-MRI from the actual liver volume obtained using MDCT 3D volumetry was calculated with the following formula.

[Actual volume (seg.X) × relative SI (seg.X) + Actual volume (seg.Y) × relative SI (seg.Y) ×100%]/[Actual volume (whole liver) × relative SI (average of whole liver)]

Immunohistochemical staining of ASGR1 and OATP. In order to elucidate the accuracy of estimation of liver functional reserve on ^{99m}Tc-GSA SPECT and EOB-MRI, we investigated the immunohistochemical expression of ASGR1 and OATP in the left and right lobe of the liver. Four out of 58 patients who underwent both left lateral and right anterior partial resections of the liver were included.

Tissue specimens of the non-tumour region in the resected liver were fixed in neutral-buffered formalin [10% v/v formalin in phosphate-buffered saline (PBS), pH 7.4] and then embedded in paraffin. The 4-μm paraffin sections were deparaffinized in xylene and rehydrated in a graded alcohol series. Endogenous peroxidase was inhibited using 3% H_2O_2 in methanol. The sections were then washed in distilled water, and heated in a microwave oven in 10 mM citrate buffer (pH 6.0) for 20 min for epitope retrieval. The slides were then incubated at 20˚C for 60 min with monoclonal antibody against ASGR1 (asialoglycoprotein receptor 1, 1:500; Sigma–Aldrich, Tokyo, Japan) and OATP (solute carrier organic anion transporter family member 1B3, 1:200; Sigma–Aldrich). The slides were incubated with anti-mouse/rabbit biotinylated bridging antibodies (1:200) (Dako, Glostrup, Denmark) for 60 min and peroxidase labelling was developed by incubating the sections in 3,3'-diaminobenzidine tetrahydrochloride for 3 min. The stained sections were reviewed using a Nikon Digital Camera DXM 1200F photomicroscope at a magnification of ×200 (×20 objectives and ×10 eyepiece).

The staining results were scored according to the percentage of positively stained cells and degree of staining (0, no staining; 1+, weak; 2+, moderate; and 3+, strong imunnohistochemical staining) as follows: H score = [3+ cells (%)×3] + (2+ cells (%)×2) + [1+ cells (%)×1] + [0 cells (%)×0] (28, 29).

Statistical analysis. All statistical analyses were performed using JMP 8.0.1 statistical software (SAS Institute, Cary, NC, USA). All data are expressed as the mean±SD. Multiple comparisons of the

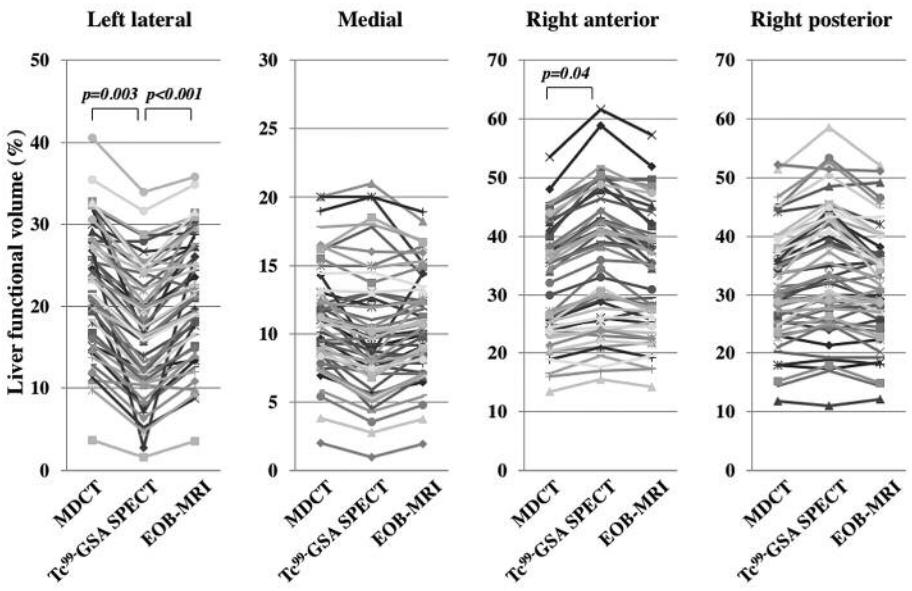

Figure 3. *Comparison of the estimated liver functional volume of each section in all patients by multidetector computed tomography (MDCT), ^{99m}Tc-galactosyl albumin single-photon-emission computed tomography (^{99m}Tc-GSA SPECT), and magnetic resonance imaging with gadoxetate-ethoxybenzyl-diethylenetriamine penta-acetic acid (EOB-MRI).*

calculated liver volume between MDCT, MDCT/^{99m}Tc-GSA SPECT and EOB-MRI formula were analysed using one-way ANOVA and the Bonferroni correction, and H score were analysed using the paired *t*-test. A value of $p<0.05$ was considered to indicate statistical significance.

Results

Functional liver volume corrected by MDCT/^{99m}Tc-GSA SPECT and EOB-MRI formula compared with actual liver volume assessment using MDCT 3D volumetry. The functional liver volume proportions of each liver section for all patients were corrected from the actual liver volumes using MDCT/^{99m}Tc-GSA SPECT fusion images and our EOB-MRI formula. The MDCT/^{99m}Tc-GSA SPECT fusion image revealed that the proportions (mean±SD) of functional liver volume were 17.1±7.6% in the left lateral section, 10.0±4.6% in the medial section, 36.0±11.3% in the right anterior section, and 34.4±10.8% in the right posterior section. The functional volumetric results using the EOB-MRI formula showed that the proportions of functional liver volume were 21.4±7.3% in the left lateral section, 10.6±3.7% in the medial section, 33.6±10.0% in the right anterior section, and 31.8±9.3% in the right posterior section.

Evaluation of the MDCT/^{99m}Tc-GSA SPECT fusion images revealed significantly lower functional liver volume in the left lateral section compared to the actual liver volume attained with MDCT 3D volumetry ($p=0.003$) and that attained using the EOB-MRI formula ($p<0.001$) (Figure 3). The functional liver volume of the right anterior section with MDCT/^{99m}Tc-GSA SPECT fusion image was significantly higher compared to the actual volume obtained with MDCT 3D volumetry ($p=0.04$) (Figure 3). In the medial and right posterior sections, there were no significant differences between the actual liver volume and the functional liver volume obtained with the MDCT/^{99m}Tc-GSA SPECT fusion images and the EOB-MRI formula. No significant differences were observed between the actual liver volume attained with MDCT 3D volumetry and the functional liver volume obtained with the EOB-MRI formula for any of the liver sections.

According to these findings, MDCT/^{99m}Tc-GSA SPECT fusion imaging might underestimate particular liver function in the left lateral section of the liver, instead overestimating those in the right anterior section of the liver. EOB-MRI gave results comparable with those of MDCT 3D volumetry. *Comparison of ASGR1 and OATP protein expression between right anterior and left lateral sections of the liver.* To confirm the discrepancy in estimation of liver function between MDCT/^{99m}Tc-GSA SPECT fusion imaging and the EOB-MRI formula results, we actually determined the expressions of ASGR1 and OATP proteins. In all, 4 out of 58 patients underwent both left lateral and right anterior partial resections of the liver, and non-tumour tissues were stained immunohistochemistry.

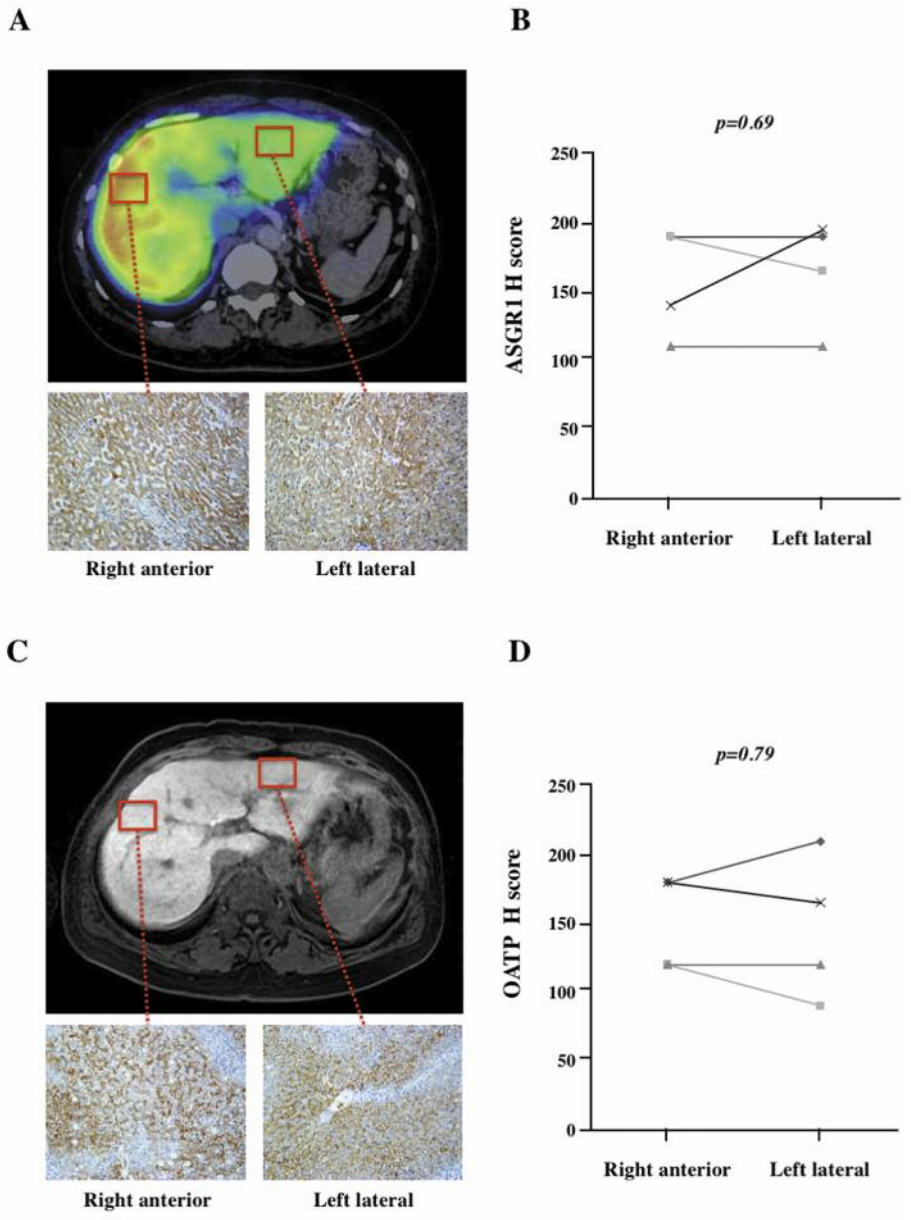

Figure 4. *^{99m}Tc-Galactosyl albumin single-photon-emission computed tomography fusion image and asialoglycoprotein receptor 1 (ASGR1) expression in liver parenchyma (A). The staining scores for ASGR1 did not significantly differ in the left lateral and right anterior sections (B). Magnetic resonance imaging with gadoxetate-ethoxybenzyl-diethylenetriamine penta-acetic acid in normal liver and ATP-dependent organic anion transporting polypeptide 1 (OATP) expression (C). OATP stained equally in the left lateral and right anterior sections (D).*

While ^{99m}Tc-GSA SPECT imaging clearly indicated a weak ROI of the left lateral section compared with the right anterior section (Figure 4A), staining scores for ASGR1 did not differ significantly between left lateral and right anterior sections of the liver (p=0.69) (Figure 4B). EOB-RI gave similar relative SIs for the left lateral and the right anterior sections, and staining scores for OATP in each section were also similar (Figure 4C and D).

Discussion

This study assessed the functional liver volume of each of four liver sections using MDCT/^{99m}Tc-GSA SPECT fusion imaging and our EOB-MRI formula. We found a significant difference particular in the functional volumetric values for the left lateral section between those obtained with MDCT/^{99m}Tc-GSA SPECT and those derived from the EOB-

MRI formula. MDCT/^{99m}Tc-GSA SPECT fusion imaging indicated significantly lower functional liver volume of the left lateral section and significantly higher functional liver volume of the right anterior section compared with the actual liver volume, while the EOB-MRI formula produced volumetric results similar to those found with MDCT 3D volumetry. Nevertheless, ASGR1 protein, which reflects hepatocyte function, was equally expressed in the left lateral and right anterior sections in our series. To our knowledge this is the first report that has indicated the utility of regional functional liver volume assessment using an EOB-MRI formula and the discrepancy between the estimated functional liver reserve using ^{99m}Tc-GSA SPECT and EOB-MRI.

EOB-MRI has recently become a standard imaging modality for patients with liver tumours in Japan (30-32). Some investigators have noted that its contrast agent, Gd-EOB-DTPA, is transported from the extracellular space into hepatocytes, following which it is secreted into biliary canaliculi. It is thus dependent on sufficient liver function, including several ATP-binding cassette transporters in the hepatocyte membranes (*e.g.* OATP, multidrug resistance-associated protein 2; MRP2). These investigators assessed the utility of liver functional reserve in both basic research and clinical settings (21-26). The relationships have been explored between Gd-EOB-DTPA enhancement of liver parenchyma at the hepatobiliary phase and several scoring systems, such as the Child-Pugh classification, the model for end-stage liver disease (MELD score, MELD-Na score), as well as indocyanine green dye (ICGR15) clearance, albumin levels, bilirubin levels, and prothrombin international normalized ratio (33-42). Other investigators have proposed that EOB-MRI offers the possibility of replacing ^{99m}Tc-GSA scintigraphy for functional assessment of the whole liver because of the significant correlation with the GSA uptake with the heart-plus-liver at 15 min (LHL15) (26, 43), as in our previous report. In an environment of increasing expectations, several MRI-based indices, liver signal-to-noise ratio (25), relative enhancement of the liver (39), increased rate of the liver-to-muscle ratio (26, 33), liver-to-muscle ratio (44), liver-to-spleen ratio (24) and T1 relaxation time (34, 35, 38) have been used to determine the most accurate assessment of liver functional reserve with EOB-MRI. Among these indices, we previously adopted the relative SI (liver-to-muscle ratio) for convenience of its measurement, and verified that the relative SI of EOB-MRI was significantly correlated with the ratio of ^{99m}Tc-GSA radioactivity of liver to that of LHL15 of ^{99m}Tc-GSA and ICGR15 (ICGR15=70.3-21.5 × relative SI) in the whole liver functional assessment (27). Moreover, the regional function of the liver in patients undergoing living-donor liver transplantation has been evaluated by EOB-MRI with the same manner of our methods (45). Therefore, in the current study, we also applied the relative SI as an MRI-based index for evaluating the regional functional liver volume.

^{99m}Tc-GSA scintigraphy is reported to be a reliable non-invasive modality for evaluating the regional hepatic functional reserve (8-11). ^{99m}Tc-GSA binds ASGR1 expressed in large quantities on the sinusoidal membrane of hepatocytes. Its liver uptake ratio, which reflects the number of functioning hepatocytes, was suitable for estimating liver function (46). Therefore, MDCT/^{99m}Tc-GSA SPECT fusion imaging technique is expected to be able to evaluate the distribution of functional hepatocytes in the entire and regional liver. However, one impressive report indicated that MDCT/^{99m}Tc-GSA fusion imaging showed decreased functional volume of the left lobe compared with the right lobe (17), as in our findings. These authors speculated that the decreased functional volume of the left lobe was attributed to lesser left portal blood supply compared with that in the right portal vein because the left portal vein branches from the right portal vein at an almost 90˚ right turn (17, 47). Our similar findings for functional liver volume assessment with MDCT/^{99m}Tc-GSA SPECT fusion imaging compelled us to further demonstrate no SI differences in each liver section with EOB-MRI and no ASGR1 or OATP protein expression difference in the left lateral and right anterior sections of the non-cirrhotic liver. In our series, the number of functioning hepatocytes might have proven to be similar in the left lateral and right anterior sections by immunohistochemistry, although it was assessed in a small number of patients. These results imply that the imaging bias of MDCT/^{99m}Tc-GSA SPECT fusion imaging was related to this discrepancy when estimating functional liver volume of the left lateral section. Another study reported that the right lobe surface showed relatively higher liver uptake density compared with the left lobe owing to depth-dependent blurring and photon attenuation in the ^{99m}Tc-GSA SPECT images (48). In addition, as MDCT and ^{99m}Tc-GSA SPECT images were performed at different times, a discrepancy in positional alignment of the liver could have adversely affected estimation of the functional liver volume (49).

Therefore, nuclear emission images in a ^{99m}Tc-GSA SPECT image should be corrected for attenuation and photon scatter in order to obtain a more accurate image. Taking our findings and previous reports together, MDCT/^{99m}Tc-GSA SPECT fusion imaging may underestimate the regional liver functional volume in left lateral section of the liver, therefore, EOB-MRI could be a reliable modality for regional functional liver assessment rather than ^{99m}Tc-GSA SPECT.

According to our results and in consideration of previous reports, we suggest that EOB-MRI may be a better method for estimating regional functional liver reserve. It also can provide a diagnostic image *via* a single MRI session for both the tumour diagnosis and estimation of regional liver function. EOB-MRI could then help hepatic surgeons to more accurately estimate the future remnant liver functional reserve after hepatectomy.

In conclusion, although various liver volume estimation techniques are currently available, it is likely that EOB-MRI is better at evaluating regional functional liver reserve and volume than ^{99m}Tc-GSA SPECT imaging.

Conflicts of Interest

The Authors declare that they have no conflict of interest in regard to this study.

References

1 Yamashita T and Kaneko S: Treatment strategies for hepatocellular carcinoma in Japan. Hepatol Res *43*: 44-50, 2013.

2 Shimada M, Takenaka K, Fujiwara Y, Gion T, Shirabe K, Yanaga K and Sugimachi K: Risk factors linked to postoperative morbidity in patients with hepatocellular carcinoma. Br J Surg *85*: 195-198, 1998.

3 Belghiti J, Hiramatsu K, Benoist S, Massault P, Sauvanet A and Farges O: Seven hundred forty-seven hepatecomies in the 1990s: an update to evaluate the actual risk of liver resection. J Am Coll Surg *191*: 38-46, 2000.

4 Taketomi A, Kitagawa D, Itoh S, Harimoto N, Yamashita Y, Gion T, Shirabe K, Shimada M and Maehara Y: Trends in morbidity and mortality after hepatic resection for hepatocellular carcinoma: an institute's experience with 625 patients. J Am Coll Surg *204*: 580-587, 2007.

5 van den Broek MA, Olde Damink SW, Dejong CH, Lang H, Malagó M, Jalan R and Saner FH: Liver failure after partial hepatic resection: definition, pathophysiology, risk factors and treatment. Liver Int *28*: 767-780, 2008.

6 Mochizuki K, Takatsuki M, Soyama A, Hidaka M, Obatake M and Eguchi S: The usefulness of a high-speed 3D-image analysis system in pediatric living donor liver transplantation. Ann Transplant *17*: 31-34, 2012.

7 Enkhbold Ch, Shimada M, Utsunomiya T, Ishibashi H, Yamada S, Kanamoto M, Arakawa Y, Ikemoto Z, Morine E and Imura S: One stop shop for 3-dimensional anatomy of hepatic vasculature and bile duct with special reference to biliary image reconstruction. Hepatogastroenterol *60*: 1861-1864, 2013.

8 Kwon AH, Matsui Y, Ha-Kawa SK and Kamiyama Y: Functional hepatic volume measured by technetium-99m-galactosylhuman serum albumin liver scintigraphy: comparison between hepatocyte volume and liver volume by computed tomography. Am J Gastroenterol *96*: 541-546, 2001.

9 Satoh K, Yamamoto Y, Nishiyama Y, Wakabayashi H and Ohkawa M: ^{99m}Tc-GSA liver dynamic SPECT for the preoperative assessment of hepatectomy. Ann Nucl Med *17*: 61-67, 2003.

10 Kaibori M, Ha-Kawa SK, Maehara M, Ishizaki M, Matsui K, Sawada S and Kwon AH: Usefulness of Tc-99m-GSA scintigraphy for liver surgery. Ann Nucl Med *25*: 593-602, 2011.

11 de Graaf W, Bennink RJ, Veteläinen R and van Gulik TM: Nuclear imaging techniques for the assessment of hepatic function in liver surgery and transplantation. J Nucl Med *51*: 742-752, 2010.

12 Sawamura T, Nakada H, Hazama H, Shiozaki Y, Sameshima Y and Tashiro Y: Hyperasialoglycoproteinemia in patients with chronic liver diseases and/or liver cell carcinoma: asialoglycoprotein receptor in cirrhosis and liver cell carcinoma. Gastroenterology *87*: 1217-1221, 1984.

13 Burgess JB, Baenziger JU and Brown WR: Abnormal surface distribution of the human asialoglycoprotein receptor in cirrhosis. Hepatology *15*: 702-706, 1992.

14 Iimuro Y, Kashiwagi T, Yamanaka J, Hirano T, Saito S, Sugimoto T, Watanabe S, Kuroda N, Okada T, Asano Y, Uyama N and Fujimoto J: Preoperative estimation of asialoglycoprotein receptor expression in the remnant liver from CT/^{99m}Tc-GSA SPECT fusion images correlates well with postoperative liver function parameters. J Hepatobiliary Pancreat Sci *17*: 673-681, 2010.

15 Yumoto Y, Yagi T, Sato S, Nouso K, Kobayashi Y, Ohmoto M, Yumoto E, Nagaya I and Nakatsukasa H: Preoperative estimation of remnant hepatic function using fusion images obtained by (99m) Tc-labelled galactosyl-human serum albumin liver scintigraphy and computed tomography. Br J Surg *97*: 934-944, 2010.

16 Beppu T, Hayashi H, Okabe H, Masuda T, Mima K, Otao R, Chikamoto A, Doi K, Ishiko T, Takamori H, Yoshida M, Shiraishi S, Yamashita Y and Baba H: Liver functional volumetry for portal vein embolization using a newly developed ^{99m}Tcgalactosyl human serum albumin scintigraphy SPECT computed tomography fusion system. J Gastroenterol *46*: 938-943, 2011.

17 Sumiyoshi T, Shima Y, Tokorodani R, Okabayashi T, Kozuki A, Hata Y, Noda Y, Murata Y, Nakamura T and Uka K: CT/^{99m}Tc-GSA SPECT fusion images demonstrate functional differences between the liver lobes. World J Gastroenterol *19*: 3217-3225, 2013.

18 Konig J, Cui Y, Nies AT and Keppler D: A novel human organic anion transporting polypeptide localized to the basolateral hepatocytes membrane. Am J Physiol Gastrointest Liver Physiol *278*: 156-1564, 2000.

19 van Montfoort JE, Stieger B, Meijer DK, Weinmann HJ, Meier PJ and Fattinger KE: Hepatic uptake of the magnetic resonance imaging contrast agent gadoxetate by the organic anion transporting polypeptide OATP1. J Pharmacol Exp Ther *290*: 153-157, 1999.

20 Takao H, Akai H, Tajima T, Kiryu S, Watanabe Y, Imamura H, Akahane M, Yoshioka N, Kokudo N and Ohtomo K: MR imaging of the biliary tract with Gd-EOB-DTPA: effect of liver function on signal intensity. Eur J Radiol *77*: 325-329, 2011.

21 Kim T, Murakami T, Hasuike Y, Gotoh M, Kato N, Takahashi M, Miyazawa T, Narumi Y, Monden M and Nakamura H: Experimental hepatic dysfunction: evaluation by MRimaging with Gd-EOB-DTPA. J Magn Reson Imaging *7*: 683-688, 1997.

22 Shimizu J, Dono K, Gotoh M, Hasuike Y, Kim T, Murakami T, Sakon M, Umeshita K, Nagano H, Nakamori S, Kato N, Miyazawa T, Nakamura H and Monden M: Evaluation of regional liver function by gadolinium-EOBDTPA-enhanced MR imaging. Dig Dis Sci *44*: 1330-1337, 1999.

23 Ryeom HK, Kim SH, Kim JY, Kim HJ, Lee JM, Chang YM, Kim YS and Kang DS: Quantitative evaluation of liver function with MRI using Gd-EOB-DTPA. Korean J Radiol *5*: 231-239, 2004.

24 Motosugi U, Ichikawa T, Sou H, Sano K, Tominaga L, Kitamura T and Araki T: Liver parenchymal enhancement of hepatocyte-phase images in Gd-EOB-DTPA-enhanced MR imaging: Which biological markers of the liver function affect the enhancement? J Magn Reson Imaging *30*: 1042-1046, 2009.

25 Tajima T, Takao H, Akai H, Kiryu S, Imamura H, Watanabe Y, Shibahara J, Kokudo N, Akahane M and Ohtomo K: Relationship between liver function and liver signal intensity in hepatobiliary phase of gadolinium ethoxybenzyl diethylene-triamine penta-acetic acid-enhanced magnetic resonance imaging. J Comput Assist Tomogr *34*: 362-366, 2010.

26 Nishie A, Ushijima Y, Tajima T, Asayama Y, Ishigami K, Kakihara D, Nakayama T, Takayama Y, Okamoto D, Abe K, Obara M, Yoshimitsu K and Honda H: Quantitative analysis of liver function using superparamagnetic iron oxide- and Gd-EOB-DTPA-enhanced MRI: comparison with technetium-99m galactosyl serum albumin scintigraphy. Eur J Radiol *81*: 1100-1104, 2012.

27 Utsunomiya T, Shimada M, Hanaoka J, Kanamoto M, Ikemoto T, Morine Y, Imura S and Harada M: Possible utility of MRI using Gd-EOB-DTPA for estimating liver functional reserve. J Gastroenterol *47*: 470-476, 2012.

28 Shi B, Abrams M and Sepp-Lorenzino L: Expression of asialoglycoprotein receptor 1 in human hepatocellular carcinoma. J Histochem Cytochem *61*: 901-9, 2013.

29 Sekine S, Ogawa R, Ojima H and Kanai Y: Expression of SLCO1B3 is associated with intratumoral cholestasis and CTNNB1 mutations in hepatocellular carcinoma. Cancer Res *102*: 1742-1747, 2011.

30 Bluemke DA, Sahani D, Amendola M, Balzer T, Breuer J, Brown JJ, Casalino DD, Davis PL, Francis IR, Krinsky G, Lee FT Jr., Lu D, Paulson EK, Schwartz LH, Siegelman ES, Small WC, Weber TM, Welber A and Shamsi K: Efficacy and safety of MR imaging with liver-specific contrast agent: U.S. multicenter phase III study. Radiology *237*: 89-98, 2005.

31 Kudo M: Will Gd-EOB-MRI change the diagnostic algorithm in hepatocellular carcinoma? Oncology *78(Suppl 1)*: 87-93, 2010.

32 Huppertz A, Balzer T, Blakeborough A, Breuer J, Giovagnoni A, Heinz-Peer G, Laniado M, Manfredi RM, Mathieu DG, Mueller D, Reimer P, Robinson PJ, Strotzer M, Taupitz M and Vogl TJ; European EOB Study Group: Improved detection of focal liver lesions at MR imaging: multicenter comparison of gadoxetic acid-enhanced MR images with intraoperative findings. Radiology *230*: 266-275, 2004.

33 Katsube T, Okada M, Kumano S, Imaoka I, Kagawa Y, Hori M, Ishii K, Tanigawa N, Imai Y, Kudo M and Murakami T: Estimation of liver function using T2* mapping on gadolinium ethoxybenzyl diethylenetriamine penta-acetic acid enhanced magnetic resonance imaging. Eur J Radiol *81*: 1460-1464, 2012.

34 Haimerl M, Verloh N, Zeman F, Fellner C, Müller-Wille R, Schreyer AG, Stroszczynski C and Wiggermann P: Assessment of clinical signs of liver cirrhosis using T1 mapping on Gd-EOB-DTPA-enhanced 3T MRI. PLoS One *8*: e85658, 2013.

35 Kamimura K, Fukukura Y, Yoneyama T, Takumi K, Tateyama A, Umanodan A, Shindo T, Kumagae Y, Ueno S, Koriyama C and Nakajo M: Quantitative evaluation of liver function with T1 relaxation time index on Gd-EOB-DTPA-enhanced MRI: comparison with signal intensity-based indices. J Magn Reson Imaging *40*: 884-889, 2014.

36 Saito K, Ledsam J, Sourbron S, Otaka J, Araki Y, Akata S and Tokuuye K: Assessing liver function using dynamic Gd-EOB-DTPA-enhanced MRI with a standard 5-phase imaging protocol. J Magn Reson Imaging *37*: 1109-1114, 2013.

37 Verloh N, Haimerl M, Zeman F, Schlabeck M, Barreiros A, Loss M, Schreyer AG, Stroszczynski C, Fellner C and Wiggermann P: Assessing liver function by liver enhancement during the hepatobiliary phase with Gd-EOB-DTPA-enhanced MRI at 3 Tesla. Eur Radiol *24*: 1013-1019, 2014.

38 Haimerl M, Verloh N, Fellner C, Zeman F, Teufel A, Fichtner-Feigl S, Schreyer AG, Stroszczynski C and Wiggermann P: MRI-based estimation of liver function: Gd-EOB-DTPA-enhanced T1 relaxometry of 3T vs. the MELD score. Sci Rep *4*: 5621, 2014.

39 Kubota K, Tamura T, Aoyama N, Nogami M, Hamada N, Nishioka A and Ogawa Y: Correlation of liver parenchymal gadolinium-ethoxybenzyl diethylenetriaminepenta-acetic acid enhancement and liver function in humans with hepatocellular carcinoma. Oncol Lett *3*: 990-994, 2012.

40 Nakamura S, Awai K, Utsunomiya D, Namimoto T, Nakaura T, Morita K and Yamashita Y: Chronological evaluation of liver enhancement in patients with chronic liver disease at Gd-EOB-DTPA-enhanced 3-T MR imaging: does liver function correlate with enhancement? Jpn J Radiol *30*: 25-33, 2012.

41 Kukuk GM, Schaefer SG, Fimmers R, Hadizadeh DR, Ezziddin S, Spengler U, Schild HH and Willinek WA: Hepatobiliary magnetic resonance imaging in patients with liver disease: correlation of liver enhancement with biochemical liver function tests. Eur Radiol *24*: 2482-2490, 2014.

42 Kim HY, Choi JY, Park CH, Song MJ, Song DS, Kim CW, Bae SH, Yoon SK, Lee YJ and Rha SE: Clinical factors predictive of insufficient liver enhancement on the hepatocyte-phase of Gd-EOB-DTPA-enhanced magnetic resonance imaging in patients with liver cirrhosis. J Gastroenterol *48*: 1180-1187, 2013.

43 Saito K, Ledsam J, Sourbron S, Hashimoto T, Araki Y, Akata S and Tokuuye K: Measuring hepatic functional reserve using low temporal resolution Gd-EOB-DTPA dynamic contrast-enhanced MRI: a preliminary study comparing galactosyl human serum albumin scintigraphy with indocyanine green retention. Eur Radiol *24*: 112-119, 2014.

44 Nojiri S, Kusakabe A, Fujiwara K, Shinkai N, Matsuura K, Iio E, Miyaki T and Joh T: Noninvasive evaluation of hepatic fibrosis in hepatitis C virus-infected patients using ethoxybenzyl-magnetic resonance imaging. J Gastroenterol Hepatol *28*: 1032-1039, 2013.

45 Ninomiya M, Shirabe K, Kayashima H, Ikegami T, Nishie A, Harimoto N, Yamashita Y, Yoshizumi T, Uchiyama H and Maehara Y: Functional assessment of the liver with gadolinium–ethoxybenzyl-diethylenetriamine penta-acetate-enhanced MRI in living-donor liver transplantation. Br J Surg *102*: 944-951, 2015.

46 Akaki S, Mitsumori A, Kanazawa S, Togami I, Takeda Y, Joja I and Hiraki Y: Technetium-99m-DTPA-galactosyl human serum albumin liver scintigraphy evaluation of regional CT/MRI attenuation/signal intensity differences. J Nucl Med *39*: 529-532, 1998.

47 Kutlu R, Karaman I, Akbulut A, Baysal T, Sigirci A, Alkan A, Aladag M, Seckin Y and Saraç K: Quantitative Doppler evaluation of the splenoportal venous system in various stages of cirrhosis: differences between right and left portal veins. J Clin Ultrasound *30*: 537-543, 2002.

48 Sugahara K, Togashi H, Takahashi K, Onodera Y, Sanjo M, Misawa K, Suzuki A, Adachi T, Ito J, Okumoto K, Hattori E, Takeda T, Watanabe H, Saito K, Saito T, Sugai Y and Kawata S: Separate analysis of asialoglycoprotein receptors in the right and left hepatic lobes using ^{99m}Tc-GSA SPECT. Hepatology *38*: 1401-1409, 2003.

49 Bybel B, Brunken RC, DiFilippo FP, Neumann DR, Wu G and Cerqueira MD: SPECT/CT imaging: clinical utility of and emerging technology. Radiographics *28*: 1097-1113, 2008.

Received July 25, 2017
Revised August 6, 2017
Accepted August 8, 2017